City Research Online

City St George's, University of London

Citation: Agrawal, A., Tiwari, M., Azabi, Y. O., Janyani, V., Rahman, B. M. & Grattan, K. T. V. (2013). Ultrabroad supercontinuum generation in tellurite equiangular spiral photonic crystal fiber. Journal of Modern Optics, 60(12), pp. 956-962. doi: 10.1080/09500340.2013.825334

This is the unspecified version of the paper.

This version of the publication may differ from the final published version. To cite this item please consult the publisher's version.

Permanent repository link: https://openaccess.city.ac.uk/id/eprint/2744/

Link to published version: https://doi.org/10.1080/09500340.2013.825334

Copyright and Reuse: Copyright and Moral Rights remain with the author(s) and/or copyright holders. Copies of full items can be used for personal research or study, educational, or not-for-profit purposes without prior permission or charge, unless otherwise indicated, provided that the authors, title and full bibliographic details are credited, a hyperlink and/or URL is given for the original metadata page and the content is not changed in any way. For full details of reuse please refer to City Research Online policy.

City Research Online: http://openaccess.city.ac.uk/ publications@citystgeorges.ac.uk

UltrabroadSupercontinuum Generation in Tellurite Equiangular Spiral Photonic Crystal Fiber

Arti Agrawal[1,*], Manish Tiwari[2], Yousaf O. Azabi[1], Vijay Janyani[3], B. M. A. Rahman[1]and K. T. V. Grattan[1]

[1]*School of Engineering and Mathematical Sciences, City University London, Northampton Square, London EC1V 0HB, United Kingdom*

[2]*Rajdhani Engineering College, Rohini Nagar Phase – I, Jaipur 303904, India*

[3]*Department of Electronics and Communication Engineering, Malaviya National Institute of Technology, Jaipur 302017, India*

We show simulations of very broad and flat Supercontinuum (SC)in both the normal and anomalous group velocity dispersion regimes of the same equiangular spiral photonic crystal fiber at low pumping powers. For the pump wavelength at 1557 nm and average pump power of 11.2 mW, we obtained a bandwidth > 3 μm (970 nm – 4100 nm) at 40 dB below the peak spectral power with fiber dispersion ~ 2.1ps/km.nm at 1557 nm. In the same fiber, at pump wavelength 1930nm and average pump power of 12mW the SC bandwidth was more than 2 octaves (1300 nm – 3700 nm) and dispersion was -1.3ps/km.nm at 1930 nm. This demonstrates the potential use of the fiber for multi-wavelength pumping with commercially available sources at fairly low power.

Keywords: Equiangular-spiral, nonlinear optics, photonic crystal fiber, supercontinuum, tellurite.

I. INTRODUCTION

Supercontinuum (SC) is generated when an optical pulse undergoes extreme broadening due to interaction of various nonlinear processes such as self – phase modulation, cross – phase modulation (XPM), self – steepening, four – wave mixing (FWM) and stimulated Raman scattering (SRS)[1]. Supercontinuum has applications in diverse fields such as frequency

*Arti Agrawal. Email:arti.agrawal.1@city.ac.uk

metrology, optical coherence tomography, spectroscopy, sensing etc. and telecom applications like pulse compression, short pulse generation, design of multi – wavelength sources, TDM to WDM conversion and vice versa and fiber characterization. Thus there is a tremendous research effort in increasing the SC bandwidth, power and flatness while lowering the input power requirements.

Photonic crystal fibers (PCFs) have become a popular choice for SC generation since the first demonstration of SCG in silica PCF[2]. The ability to obtain large nonlinearity (γ), and flat dispersion near the pump wavelength make PCF the preferred option for SCG.

Nonlinearity, ($\gamma = 2\pi n_2/\lambda A_{eff}$) is one of the most important factors governing the spectral broadening of optical pulses. The overall width of SC is restricted by the nonlinear refractive index (n_2=2.2 x 10^{-20} m^2/W) in case of silica fibers. Also, the small transmission window of silica glasses (0.2-3 μm) limits the SC generation beyond this range. This limitation has attracted attention towards non – silica glasses such as lead – silicate[3], fluoride[4], chalcogenide[5], and tellurite[6-8] glasses that have larger n_2 and some of which are transparent in the mid – infrared window.

Tellurite glasses have a large nonlinear refractive index (n_2=2 – 6 x 10^{-19} m^2/W), wide transmission range (0.35 - 5 μm), good glass stability, good corrosion resistance and low phonon energy[9]. These properties imply that tellurite fibers can be excellent for nonlinear applications.

Another important fiber characteristic that affects nonlinearity (and thus SC) is the effective modal area, A_{eff}. A highly confined mode with small A_{eff} will yield larger γ. Therefore, special attention is paid in designing PCF with small A_{eff} and examples include the triangular core (TC) fibers[10], wagon wheel PCF[11] and multi – ring fibers[12]. It has been shown previously, that the Equiangular Spiral PCF (ES – PCF) has extremely well confined modal field with small A_{eff}[13].

Finally, the dispersion of the fiber plays an important role in determining the SC spectrum. Ideally the dispersion near the pump wavelength ought to be small in magnitude as well as relatively flat[14]. In TC designs due to small core and large index contrast, the effective modal index of the guided mode changes rapidly with wavelength, yielding large dispersion slope that can be difficult to flatten with the limited number of design parameters. Conventional PCF designs can allow for better dispersion control through engineering of the cladding microstructure, but with lower nonlinearity. Therefore, it is not easy to achieve both desired dispersion and non-linearity. However, the ES-PCF can simultaneously yield large nonlinearity with flat and small, anomalous dispersion. This is due to the special properties of the ES-PCF: the bridge regions of high refractive index between the air holes are much smaller and narrower than in the conventional hexagonal PCF (distance between second and first ring holes is about 0.49 times the pitch for ES-PCF as compared to 0.87 for conventional PCF). Furthermore, the second ring is rotated with respect to the first ring such that the field is prevented from spreading through the silica regions between air holes more effectively than conventional PCF. The dispersion is much flatter and low compared to TC designs where even slight change in wavelength leads to the field expanding outside the core rapidly (and thus suffering from large dispersion). In ES-PCF as the field spreads out farther and interacts with the glass in the region beyond the first ring of air-holes, the change in effective index of the mode is slow and dispersion remains flat.The ES – PCF is able to simultaneously offer large γ as well as flat dispersion in the wavelength range of interest[13], therefore in this paper we consider SCG in tellurite ES – PCF. The fabrication of the ES – PCF has been discussed in a letter as well[15].

We demonstrate SC that is extremely broadband and flat at very low pump powers at 1550nm and 1930 nm. To our knowledge this may be one of the few studies that reports SCG in both the normal and anomalous Group Velocity Dispersion (GVD) regimes of the same

fiber at such low pump powers. The application of such broadband SCG is promising for astronomical applications as well as in spectroscopy of bio-chemical species.

The paper is organized as follows: in Section II we present the fiber design and its modal properties including dispersion. Section III a presents the results for numerical simulation of SCG with the Generalized Non-Linear Schrödinger Equation (GNLSE) for pumping the fiber at 1557 nm. Section III b contains the results for SCG pumped at 1930nm. The conclusion contains the discussion of all these results and findings.

II. TELLURITE ES - PCF: DESIGN AND OPTICAL PROPERTIES

The equation for the ES shown in Figure 1 (a) in polar coordinates is:

$$r = r_o e^{\theta \cot \alpha} \tag{1}$$

where r_o is the spiral radius (distance from center of structure to the center of air holes in 1st ring), θ is the angular increment (angle between two successive air holes in the same arm), r is the distance between the center of any air hole and the center of the structure, α is the angle between the tangent and the radial line.

The structure of the fiber that we present here is a modification of the ES-PCF reported earlier[13]. The radii of the air holes in ring 1, 2 and 3 are r_1, r_2 and r_3 respectively, with ring 1 being the innermost ring and ring 3 being the outermost. The arrangement of air holes in the ES – PCF is as shown in Figure 1 (b).

In the ES – PCF, air holes of each ring are rotated with respect to the previous ring. This effectively stops the field from spreading into regions between air holes and confines the mode tightly in the core area. The ES – PCF parameters used in this paper are: 3 ring, 6 arm structure with spiral radius,r_0 = 0.75 µm, spiral angle, θ = 30^o and hole radius r_1, r_2 *and* r_3 equal to 0.1, 0.22 and 1.2134 µm respectively. We expect that the ES-PCF can also be

fabricated by the new extrusion techniques that are being applied to realize challenging structures in soft glass such as TC fibers[10].

FIG. 1.(a) Equiangular spiral constructed using Eq. (1) (b) The structure of the ES – PCF.

The tellurite glass used in this work is 76.5TeO_2-6Bi_2O_3-11.5Li_2O-6ZnO (mol%)[12,16]. The nonlinear refractive index $n_2$of this tellurite glass is 5.9 x 10^{-19} m^2/W[12]. The refractive index of this tellurite glass is calculated by Sellmeier's equation $n^2 = 1 + \sum_{i=1}^{i=3}[A_i\lambda^2/(\lambda^2 - L_i^2)]$. Table 1 gives the values of fitting coefficients A_i and L_i[17].

TABLE I: Sellmeier coefficients for the tellurite glass

i	A_i	L_i^2
1	1.67189	0.0004665
2	1.34862	0.0574608
3	0.62186	46.72542736

The fiber was characterized using a full – vector FEM[18]. Figure 2 shows the field profile of the fundamental mode in the fiber at 1557 nm.

FIG. 2.Field profile of the fundamental mode at 1.557 μm.

Figure 3 shows both the material and the total dispersion variation with wavelength. Fundamental mode of propagation has been considered to find the dispersion characteristics of the fiber. Material dispersion for the entire wavelength range has been calculated using the Sellmeier's coefficients given in Table I. The material dispersion values range from ~75 ps/km/nm @ 1.5 μm to 100 ps/km/nm @ 2.5 μm and the Zero Dispersion Wavelength (ZDW) is at ~1.84 μm whereas the total dispersion in ES – PCF remains very flat. The inset of Figure 3 shows a graph of the total dispersion from 1.5 μm – 2.3 μm, where it varies very little, in the range of ±4 ps/nm/km. In addition, the ES – PCF exhibits three ZDWs at 1.52, 1.88 and 2.22μm which can make multi – wavelength pumping possible and the dispersion

slope is less than 0.003 ps/nm^2/km in the range 1.5 – 2.3 μm. This is an extremely desirable condition for SCG, as low and flat dispersion in tellurite PCF is not easy due to the large refractive index which causes rapid effective index variation with wavelength. However, the ES-design allows us to optimize the modal field properties and obtain ultra-flat dispersion in a very large wavelength range of ~ 800 nm.

FIG. 3.Material and total dispersion of the tellurite ES-PCF. The inset shows the total dispersion in IR –B band (ZDWs at 1.52, 1.88 and 2.22 μm).

FIG. 4.Nonlinearity of the tellurite ES-PCF.

Figure 4 depicts the variation in the nonlinearity of the ES – PCF with respect to wavelength. The nonlinearity is very high ranging from 4650 W^{-1} km^{-1} @ 800 nm to 655 W^{-1} km^{-1} @ 2.5 μm. At the pump wavelength of 1557 nm, the value of nonlinearity, γ is 1740 W^{-1} km^{-1}.

These dispersion and γ values compare favorably with[17] where in γ was 394 W^{-1} km^{-1} and dispersion was~75 ps/km/nm @ 1557 nm. The effect of γ and dispersion will be clearly visible on the SC generated and is discussed in the following section.

III. SUPERCONTINUUM GENERATION

In this section, we discuss briefly the methodology for SCG and the results obtained for SCG in the tellurite ES- PCF.

The SC is modeled by solution of the GNLSE.

$$\frac{\partial A}{\partial z} = -\frac{\alpha}{2}A + \sum_{n\geq 2}\frac{i^{n+1}}{n!}\beta_n\frac{\partial^n A}{\partial T^n} + i\gamma\left(1+\frac{i}{\omega_0}\frac{\partial}{\partial T}\right).\int_{-\infty}^{\infty} R(T')\left|A(z,T-T')\right|^2 dT' \qquad (2)$$

where

A(z,t): the envelope of the optical field,

T: time,

α : = the fiber loss coefficient ([1/m])

β_n: the n^{th} derivative of the propagation constant β

γ: the nonlinear coefficient.

The nonlinear response function *R(T)*, which includes instantaneous electronic as well as delayed Raman contributions is given by

$$R(T) = (1 - f_r)\delta(T) + f_r h_r(T) \tag{3}$$

where f_r=0.51 for this tellurite glass[18] and we have calculated $h_r(T)$ by a similar method[19].The split-step Fourier method has been used to solve the GNLSE[1].

A. Pump wavelength = 1557 nm

We first consider the simulation of SCG at the pump wavelength of 1557 nm. We consider the same parameters as Ref. 12: ultrashort laser pulses of hyperbolic secant in shape with a peak power of 1670 W, width T_0= 400 fs at 1557 nm and a repetition rate of 16.75 MHz. The length of the fiber has been taken as 10 cm. We use a value of 10 dB/m for loss in our calculations as this is the much higher than the reported loss value for tellurite PCF[12] at the target pump wavelength.

FIG. 5. Pulse evolution through the ES – PCF (Spectral domain).

The relative position of the pump wavelength (1557 nm) with respect to the ZDW is an important factor for the spectral broadening in the SC generation[20]. The spectrum can be further broadened by shifting the pump away from the ZDW but this leads to a drastic reduction of the blue-wavelength components[20,14]. Therefore the location of first ZDW (1520 nm) which is closer to the pump wavelength is suitable for a flat and broad SCG.

Figure 5 shows the SC spectra as the pulse propagates through the fiber. It can be seen that during the initial phase of its propagation, the pulse undergoes a symmetrical spectral broadening under the effect of self phase modulation during first 1.5 cm. During this time, the

pulse also undergoes temporal compression. Self Phase Modulation (SPM) induces large amount of frequency chirp on the pulse making it very sensitive to GVD perturbation. These dispersive effects, though very weak, lead to a phenomenon called optical wave breaking wherein the pulse spectrum becomes nearly rectangular with spectral side lobes and a linear chirp across its entire width which can be seen in Figure 5 at length = 1 cm. But after this, the broadening becomes asymmetric and the asymmetry increases as the pulse propagates further. The long wavelength components are continuously redshifted whereas the short wavelength components do not extend further with propagation. The overall width of supercontinuum achieved here is > 3 μm (970 nm – 4100 nm) with 11.2 mW of average pump power at a shorter length of fiber (10 cm) in comparison to ~ 1600 nm with same pump characteristics in[12]. After 10 cm, there is a very little pulse broadening. Only redistribution of energy takes place over the bandwidth achieved. Furthermore, in the work of other groups, example, Domachuk et al.[7] and Qin et. al.[4], very large bandwidth SC has been demonstrated. However, this SC has been obtained at much larger pump power than what we report here, Domachuk et al. report using pulses of ~ 8kW peak power and Qin et al.[4] reported a SC spanning ultraviolet to 6.28 μm at 1450 nm using peak pulse power of 0.4 MW, while our results are for only 1.67 kW of peak power.

FIG. 6. Spectral and temporal evolution of the pulse through the ES – PCF (a) f_R =0.51 (b) f_R= 0.

Figure 6 (a) and (b) show the spectral and temporal evolution of the pulse in the presence and absence of Raman scattering respectively. In presence of Raman scattering, the pulse splits into fundamental solitons with high amplitude, which then shift to longer wavelengths through self – frequency shift seeding the generation of both short and long wavelength components. This leads to the distribution of energy in a wider spectrum. However, in absence of Raman effect, the energy of the solitons ejected is not high enough to

seed the generation of spectral components in long wavelength region. Thus, the pulse energy is more concentrated around the pump wavelength and less energy is distributed in both anomalous and normal GVD region which limits the bandwidth of the entire SC spectrum.

FIG. 7.Power dependent supercontinuum spectra of tellurite ES – PCF pumped by a femtosecond fiber laser. The curve is displaced by 40 dB.

Figure 7 shows the power dependent spectra of supercontinuum generated in tellurite ES – PCF using femtosecond source at 1557 nm with 400 fs pulses. The vertical line in the plot shows the pump wavelength of laser source. The average pump power was varied from 0.7 mW to 11.2 mW. The width of SC spectrum is controlled by pump power and here we are able to achieve three octave spanning supercontinuum with average pump power much lesser than 15mW. The flatness and width of the SC spectra are due to the flattened dispersion and high nonlinearity of the fiber. Moreover, due to extremely short length of the fiber, the optical losses should not pose much problem in generation of a broad SC spectrum.

B. Pump wavelength = 1930 nm

We now investigate SCG in the same fiber, but pumped at 1930nm. We have launched ultrashort pulses with a peak power of 3000 W, width T_0= 100 fs at 1930 nm at a repetition rate of 40 MHz. We have chosen this pump wavelength due to availability of high – gain thulium mode-locked lasers in wavelength range of 1.8 – 2.1 μm. The nonlinearity of the fiber at 1930 nm is 1155 m^2/W. We have taken a 3 cm long fiber length in our simulations.

Figure 8 (a) shows the spectral and temporal evolution of the pulse in the fiber. Initially, SPM and GVD interact together while the pulse broadens in normal GVD region. Due to this broadening, the spectral components are generated near third ZDW (2220 nm) and across the anomalous dispersion. This process causes solitons dynamics to come into play and a rapid transfer of energy to longer wavelengths can be observed after the soliton

fission that takes place at ~5 mm. After this, Raman shift can be seen in the spectrum due to Raman perturbation and clear signatures of soliton fission and dispersive wave generation can be observed in both temporal and spectral SC characteristics. However, the higher order dispersion influences the propagation of Raman soliton. It reduces the solitons self – frequency shift and thus limits propagation of solitons and leads to generation of dispersive waves.

FIG. 8.(a) Pulse evolution through the ES – PCF at pump wavelength = 1930 nm. (b) Pulse spectrum at the end of the fiber

Figure 8 (b) shows that the overall width of the supercontinuum generated is almost two octave (1300 nm – 3700 nm) at 40 dB below the peak pulse power. Though comparable and even larger bandwidth have been reported in the literature, for example, Buccoliero et. al.[8] reported SC using average power of 15 W, while we report here is using average power of 12 mW. Thus for an average pump power value that is lower by almost three orders of magnitude, the SC bandwidth obtained in the ES-PCF is substantial and is quite flat.

IV. CONCLUSION

In this paper, we have presented a highly nonlinear tellurite ES – PCF with three zero dispersion wavelengths at 1520, 1880 and 2220 nm. The fiber has ultraflat dispersion profile and very high nonlinearity at target pump wavelengths 1557 nm (γ = 1740 m^2/W) and 1930 nm (γ = 1155 m^2/W). This combination of extremely desirable fiber characteristics make the fiber a potential candidate for development of compact and low – cost supercontinuum sources. We have demonstrated the suitability of the fiber for relatively low pump power SC generation using pump sources available at 1.55 μm and 1.93 μm. The SC extends from 970 nm to 4100 nm i.e. three octave, with a 10 cm fiber and ~11.2 mW of average pump power when pumped at 1550nm. The same fiber shows SC spanning almost two octaves (1300 nm

– 3700 nm) when pumped at the thulium wavelength of 1930 nm with pump pulses of average power of 12 mW with a short length of fiber (3 cm). These results show that the same fiber can be used to generate SC pumped at two pump wavelengths that are far apart: 1550 and 1930 nm and in different dispersion regimes, at low pump powers.

ACKNOWLEDGMENT

The authors would like to thank the UKIERI Major Grant on microstructured optical fibers for support.

REFERENCES

[1] G. P. Agarwal, *Nonlinear Fiber Optics-4e*. (Academic, 2007).
[2] J. K. Ranka, R. S. Windeler, and A. J. Stentz, "Visible continuum generation in air-silica microstructure optical fibers with anomalous dispersion at 800 nm," Opt. Lett.**25**, 25–27, (2000).
[3] M. Tiwari and V. Janyani, "Two-Octave Spanning Supercontinuum in a Soft Glass Photonic Crystal Fiber Suitable for 1.55 μm Pumping," J.Lightw. Technol.**29** (23), 3560-3565, (2011).
[4] G. Qin, X. Yan, C. Kito, M. Liao, C. Chaudhari, T. Suzuki, and Y. Ohishi, "Ultra-Broadband Supercontinuum Generation from Ultraviolet to 6.28 μm in a Fluoride Fiber," Appl. Phys. Lett. **95**, 161103 (2009).
[5] T.M. Monro, Y.D. West, D. W. Hewak, N. G. R. Broderick, and D. J. Richardson, "Chalcogenide holey fibers," Electron. Lett.**36** (24), 1998–2000, (2000).
[6] V. Kumar, A. K. George, J. C. Knight, and P. S. Russell, "Tellurite photonic crystal fiber," Opt. Exp.**11**, 2641–2645, (2003).
[7] P. Domachuk, N. A. Wolchover, M. Cronin-Golomb, A. Wang, A. K. George, C. M. B. Cordeiro, J. C. Knight, and F. G. Omenetto, "Over 4000 nm bandwidth of mid-IR supercontinuum generation in sub-centimeter segments of highly nonlinear tellurite PCFs," Opt. Express **16** (10), 7161–7168 (2008).
[8] D. Buccoliero, H. Steffensen, O. Bang, H. Ebendorff-Heidepriem, and T. M. Monro, "Thulium pumped high power supercontinuum in loss-determined optimum lengths of tellurite photonic crystal fiber," Appl. Phys. Lett. **97**, 061106 (2010).
[9] J. S. Wang, E. M. Vogel, and E. Snitzer, "Tellurite glass: new candidate for fiber devices," Opt. Mater. **3** (3), 187–203 (1994).
[10] J. Y. Y. Leong, P. Petropoulous, J. H. V. Price, H. Ebendorff-Heiderpriem, S. Asimakis, R. C. Moore, K. Frampton, V. Finazzi, X. Feng, T. M. Monro, and D. J. Richardson, "High-nonlinearity dispersion-shifted lead-silicate holey fibers for efficient 1- μm pumped supercontinuum generation," J. Lightw. Technol. **24** (1), 183–190, (2006).
[11] V. Finazzi, T. M. Monro, and D. J. Richardson, "Small-core silica holey fiber: Nonlinearity and confinement loss trade-offs," J. Opt. Soc. Amer. B **20** (7), 1427–1436, (2003).
[12] M. Liao, X. Yan, G. Qin, C. Chaudhari, T. Suzuki, and YasutakeOhishi, "A highly non-linear tellurite microstructure fiber with multi-ring holes for supercontinuum generation," Opt. Exp. **17**, 15481-15490 (2009).
[13] A. Agrawal, N. Kejalakshmy, B. M. A. Rahman, and K. T. V. Grattan, "Soft glass equiangular spiral photonic crystal fiber for supercontinuum generation," IEEE Photon. Tech. Lett.**21** (22), 1722–1724, (2009).
[14] G. Genty, M. Lehtonen, H. Ludvigsen, J. Broeng, and M. Kaivola, "Spectral broadening of femtosecond pulses into continuum radiation in microstructured fibers," Opt. Exp.**10**, 1083–1098, (2002).
[15] Arti Agrawal, Y. O. Azabi and B.M.A. Rahman, "Stacking the equiangular spiral", IEEE Photon. Tech. Lett., **25**, 291-294, (2013).
[16] M. Liao, C. Chaudhari, G. Qin, X. Yan, C. Kito, T. Suzuki, Y. Ohishi, M. Matsumoto, and T. Misumi, "Fabrication and characterization of a chalcogenide-tellurite composite microstructure fiber with high nonlinearity," Opt. Exp. **17**, 21608-21614 (2009)

[17] C. Chaudhari, T. Suzuki and Y. Ohishi, "Chalcogenide Core Photonic Crystal Fibers for Zero Chromatic Dispersion in the C-Band," OSA/OFC/NFOEC, OTuC4 (2009).
[18] N. Kejalakshmy, B. M. A. Rahman, A. Agrawal, T. Wongcharoen and K. T. V. Grattan, "Characterization of single-polarization single-mode photonic crystal fiber using full-vectorial finite element method," Appl. Phys. B **93,** 223-230 (2008).
[19] X. Yan, G. Qin, M. Liao, T. Suzuki, Y. Ohishi, "Raman response function for tellurite fibers," 23rd Annual Meeting of the IEEE Photonics Society, 2010 , pp.677-678, 7-11 Nov. 2010.
[20] G. Genty, M. Lehtonen, H. Ludvigsen, and M. Kaivola, "Enhanced bandwidth of supercontinuum generated in microstructured fibers," Opt. Exp. **12**, 3471–3480, (2004).

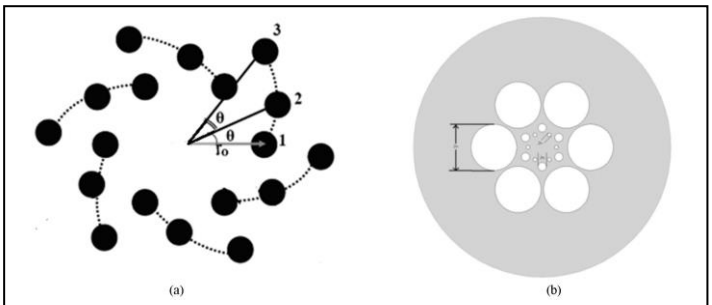

Figure 1

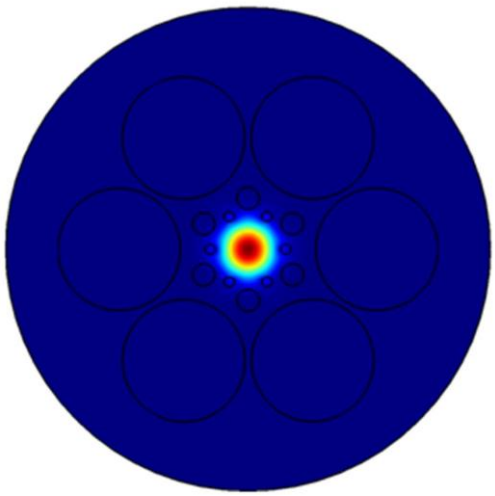

Figure 2

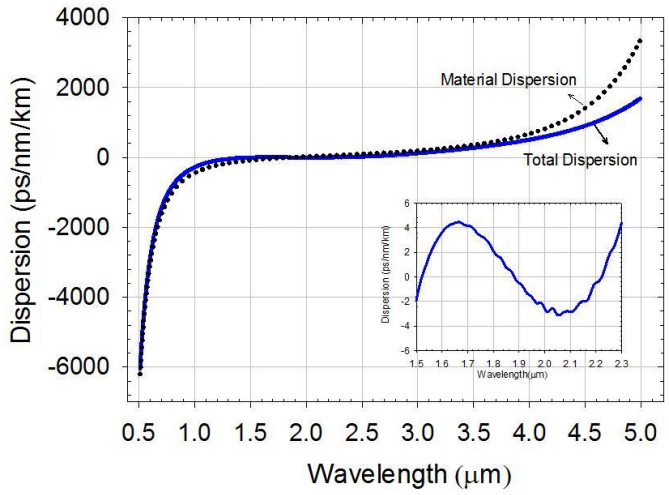

Figure 3

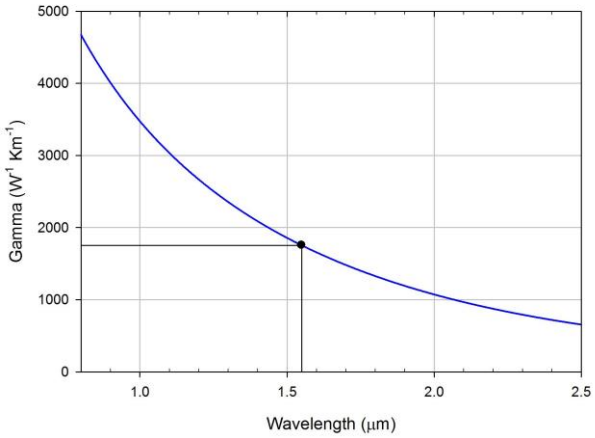

Figure 4

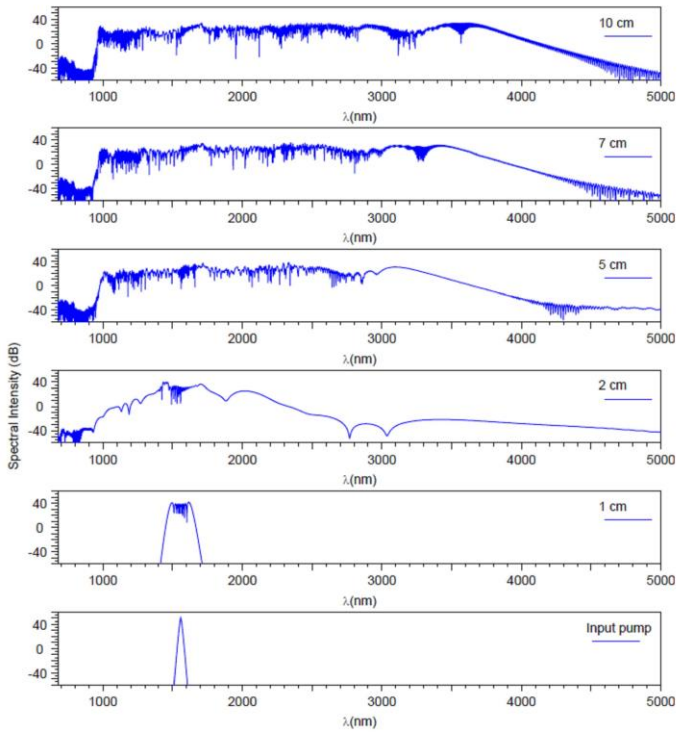

Figure 5

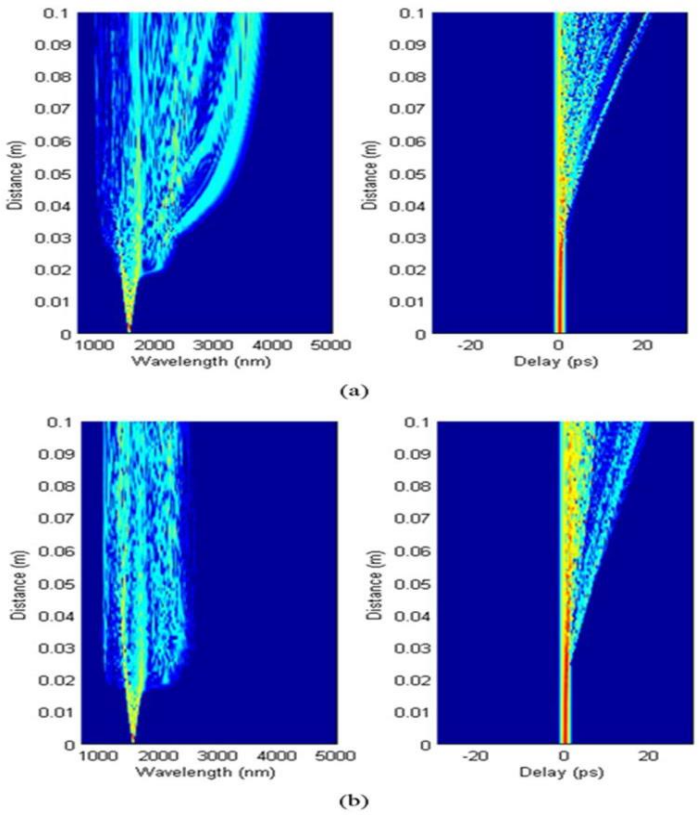

Figure 6

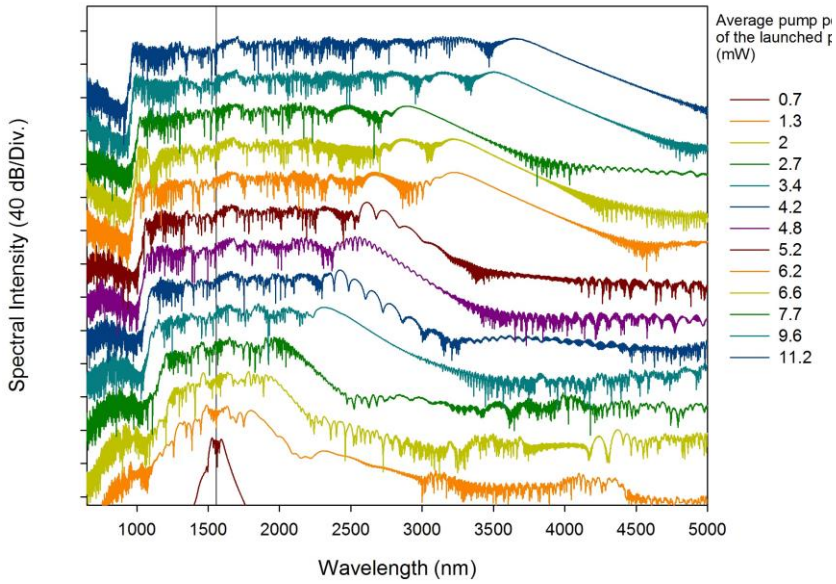

Figure 7

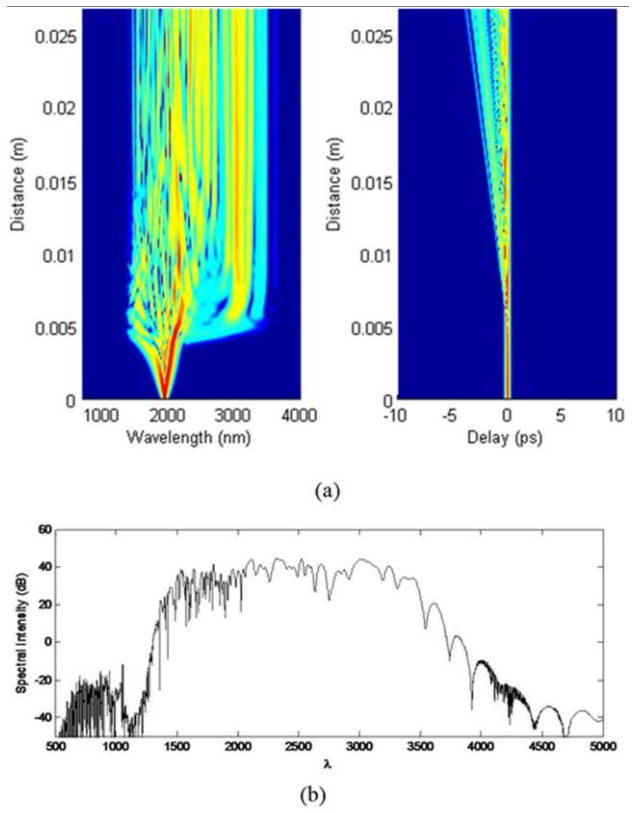

Figure 8